

# DexDiffuser: Generating Dexterous Grasps with Diffusion Models

Zehang Weng\*, Haofei Lu\*,<sup>†</sup>, Danica Kragic, and Jens Lundell  
Division of Robotics, Perception, and Learning (RPL), KTH  
{zehang,haofei,dani,jelundel}@kth.se

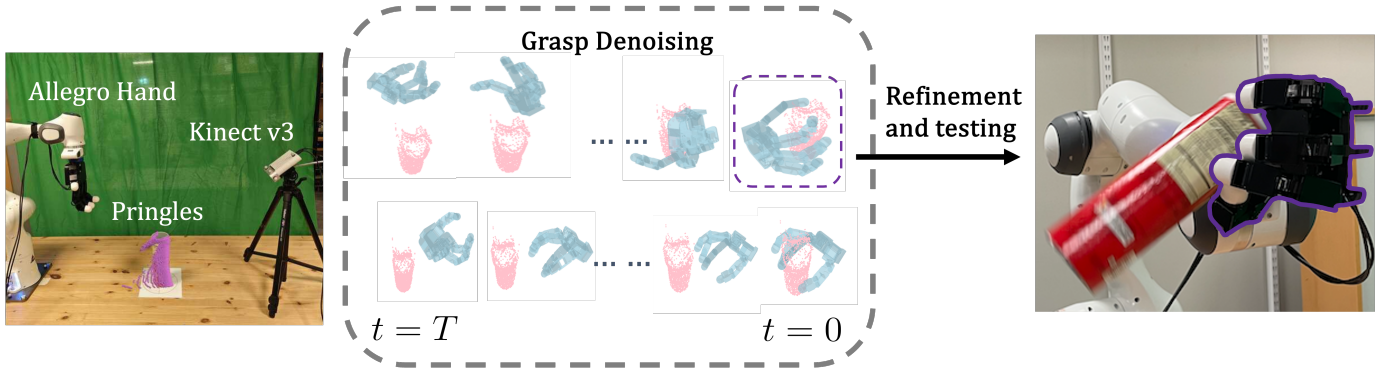


Fig. 1: DexDiffuser. Given a partial point cloud captured by a Kinect v3, DexSampler generated a set of high-quality grasps by gradually removing noise from randomly sampled grasps. Subsequently, the grasps were refined and ranked using DexEvaluator. The grasp with the highest score was finally selected and executed successfully on the real robotic hardware.

**Abstract**—We introduce DexDiffuser, a novel dexterous grasping method that generates, evaluates, and refines grasps on partial object point clouds. DexDiffuser includes the conditional diffusion-based grasp sampler DexSampler and the dexterous grasp evaluator DexEvaluator. DexSampler generates high-quality grasps conditioned on object point clouds by iterative denoising of randomly sampled grasps. We also introduce two grasp refinement strategies: Evaluator-Guided Diffusion and Evaluator-based Sampling Refinement. Our simulation and real-world experiments on the Allegro Hand consistently demonstrate that DexDiffuser outperforms the state-of-the-art multi-finger grasp generation method FFHNet with an, on average, 21.71–22.20% higher grasp success rate.

## I. INTRODUCTION

Despite years of research on data-driven grasping [24], generating dexterous grasps for picking unknown objects, similar to the example shown in Fig. 1, remains challenging [20]. What makes dexterous grasping particularly difficult is identifying successful grasps within a high-dimensional search space where unsuccessful grasps far outnumber successful ones.

In this work, we propose the new data-driven dexterous grasping method DexDiffuser to address the dimensionality issue. DexDiffuser includes DexSampler, a new conditional diffusion-based dexterous grasp sampler, and DexEvaluator, a new dexterous grasp evaluator. DexSampler generates high-quality grasps conditioned on object point clouds by iteratively denoising randomly sampled grasps. In addition to

DexDiffuser, we also propose two grasp refinement strategies Evaluator-Guided Diffusion (EGD) and Evaluator-based Sampling Refinement (ESR) that use the DexEvaluator to improve the grasps.

We experimentally assess DexDiffuser’s capability to sample, evaluate, and refine 16-Degrees of Freedom (DoF) Allegro Hand grasps on three visually and geometrically distinctive object datasets in simulation and on one dataset in the real world. DexDiffuser is benchmarked against the state-of-the-art multi-finger grasp generation method FFHNet [20]. The experimental results indicate that our best method achieves a grasp success rate of 91.43% in simulation and 68.89% in the real world, which is 29.79% and 33.33% higher than the respectively best FFHNet model.

Our contribution can be summarized as follows:

- DexSampler the novel diffusion-based dexterous grasp sampler (Section IV-B), and DexEvaluator the dexterous grasp evaluator (Section IV-C).
- The two refinement strategies EGD and ESR for improving dexterous grasps (Section IV-D).
- An algorithm for extending dexterous grasping datasets that only contains successful grasps with unsuccessful ones (Section V).
- A comprehensive experimental evaluation demonstrating the efficacy and real-world applicability of DexDiffuser (Section VI).

\*These authors contributed equally to this work

<sup>†</sup>Corresponding author

## II. RELATED WORK

This work spans two topics: data-driven dexterous grasping and diffusion models. For brevity, we limit the related works of diffusion models to robotic applications and, for other areas, refer to the comprehensive survey by Yang et al. [39].

### A. Data-Driven Dexterous Grasping

Data-driven dexterous grasp sampling methods primarily fall into three categories: 1) those that generate a contact map on the object’s surface [9, 13, 38], 2) those that rely on shape completion [26, 16, 17, 35, 14, 15, 10, 37], or 3) those that train a grasping policy based on Reinforcement Learning (RL) [29, 19] or human demonstrations [36]. The main limitation of the methods in 1) is the assumption of complete object observation, which hinders real-world applications where complete visibility cannot be guaranteed. Methods in 2) are limited because the generated grasp quality is closely intertwined with the completion quality while collecting expensive demonstrations, and the sim-to-real gap limits the methods in 3).

Only a few methods [4, 20] do not adhere to any of the above categories as they generate grasp poses directly on incomplete object observations without shape completion nor training a grasping policy. To make learning more tractable, Choi et al. [4] only considered one gripper configuration and discretized the possible SE(3) grasp poses into 6 different approach directions and 4 orientations. They then trained a discriminative network to score which of the 24 pre-selected grasp poses had the highest grasp success probability.

In comparison, Qian et al. [20] proposed FFHNet: a Variational Autoencoder (VAE)-based grasp sampler that generates 15-DoF gripper configurations and grasp poses in all of SE(3). Unfortunately, FFHNet was only evaluated in simulation, leaving the question of real-world performance unanswered. Similar to FFHNet [20], DexDiffuser also produces complete gripper configurations and SE(3) grasp poses but does that using diffusion models. Also, we experimentally validate DexDiffuser and FFHNet on real robotic hardware.

### B. Diffusion Models in Robotics

Despite being in its infancy, diffusion models have already found widespread applicability in robotics. Some success stories include motion planning [1], navigation [31], manipulation [3, 12, 33, 2], human-robot interaction [25] and grasping [34]. Of these, the most related to ours is the grasping work by Urain et al. [34], where a diffusion model was trained to generate SE(3) parallel-jaw grasp poses. We, however, propose a diffusion model for generating *dexterous* grasps, meaning that *both* SE(3) grasp poses and high dimensional gripper configurations are generated.

Prior works on diffusion models in robotics have also trained discriminators to evaluate the diffusion-generated samples [12, 33]. In [12], the discriminator scores how realistic point cloud-generated scenes are, while the discriminator in [33] scores how good a generated SE(3) pose is for manipulating an object. Similarly, we use a discriminator to evaluate a generated grasp’s success probability in picking an object.

## III. PROBLEM STATEMENT

We consider the problem of sampling and evaluating dexterous grasps  $\mathbf{G}$  on partially observed point clouds  $\mathbf{O} \in \mathbb{R}^{N \times 3}$  for the task of successfully picking up objects. In this work, a grasp  $\mathbf{g} \in \mathbf{G} = [\mathbf{r}, \mathbf{p}, \mathbf{q}] \in \mathbb{R}^{9+k}$  is represented by a continuous 6-D rotation vector  $\mathbf{r} \in \mathbb{R}^6$  [40], a 3-D position  $\mathbf{p} \in \mathbb{R}^3$ , and a gripper joint configuration  $\mathbf{q} \in \mathbb{R}^k$ . Henceforth,  $\mathbf{r}$  and  $\mathbf{p}$  are together referred to as the grasp pose and  $\mathbf{q}$  as the joint angles. We assume all objects are reachable and singulated, and the object point cloud is segmented from the scene.

We frame the problem of sampling grasps as learning a distribution  $P(\mathbf{g} \in \mathbf{G} | \mathbf{O})$  and of evaluating grasps as learning a discriminator  $P(S = 1 | \mathbf{g}, \mathbf{O})$ , where  $S$  is a binary variable representing grasp success ( $S=1$ ) and failure ( $S=0$ ). Henceforth,  $P(S = 1 | \mathbf{g} \in \mathbf{G}, \mathbf{O})$  is referred to as the grasp evaluator and  $P(\mathbf{g} \in \mathbf{G} | \mathbf{O})$  as the grasp generator. We approximate each of these distributions with a separate Deep Neural Network (DNN)  $\mathcal{D}_\theta(\mathbf{g} \in \mathbf{G} | \mathbf{O}) \approx P(\mathbf{g} \in \mathbf{G} | \mathbf{O})$  and  $\mathcal{D}_\psi(S = 1 | \mathbf{g} \in \mathbf{G}, \mathbf{O}) \approx P(S = 1 | \mathbf{g} \in \mathbf{G}, \mathbf{O})$ , with learnable parameters  $\theta$  and  $\psi$ . The objective then becomes learning  $\theta$  and  $\psi$  from data.

## IV. METHOD

We now introduce our framework DexDiffuser to learn the parameters  $\theta$  and  $\psi$ . DexDiffuser consists of two parts: DexSampler and DexEvaluator. We also propose two grasp refinement strategies for improving the grasp success probability.

### A. The Basis Point Set (BPS) Representation

DexDiffuser generates and samples grasps directly on partial object point clouds. In this work,  $\mathbf{O}$  is encoded into  $\mathbf{f}_\mathbf{O}$  using BPS [27] as this encoding has shown to work well in prior dexterous grasping work [20]. The BPS encoding represents the shortest distance between each point in a fixed set of basis points and all points in  $\mathbf{O}$ . The benefit of BPS is that it captures the shape and spatial properties of the object and is of fixed length, which allows for the use of computationally efficient Fully Connected (FC) layers to further process  $\mathbf{f}_\mathbf{O}$ .

### B. Grasp Sampler

DexSampler is a classifier-free, conditional diffusion model that generates  $\mathbf{G}$  conditioned on  $\mathbf{f}_\mathbf{O}$ . It consists of a forward process that gradually turns data into Gaussian noise and a learnable inverse diffusion process that recovers the data from noise given the condition [5].

In our case, the forward process for incrementally diffusing a successful grasp  $\mathbf{g}_0 = [\mathbf{r}_0, \mathbf{p}_0, \mathbf{q}_0]$  over  $T$  timesteps is

$$q(\mathbf{g}_{1:T} | \mathbf{g}_0) = \prod_{t=1}^T q(\mathbf{g}_t | \mathbf{g}_{t-1}), \quad (1)$$

$$q(\mathbf{g}_t | \mathbf{g}_{t-1}) = \mathcal{N}(\mathbf{g}_t; \sqrt{1 - \beta_t} \mathbf{g}_{t-1}, \beta_t \mathbf{I}), \quad (2)$$

where  $\beta_t$  is the scheduled noise variance at time step  $t$ . To recover the original  $\mathbf{g}_0$  from  $\mathbf{g}_T$ , DexSampler needs to iteratively estimate the Gaussian noise added at each time step  $t$  in order to remove it. We propose the following parametric noise predictor  $\epsilon_\theta$  that estimates the mean  $\hat{\mu}_t$  and variance  $\hat{\Sigma}_t$

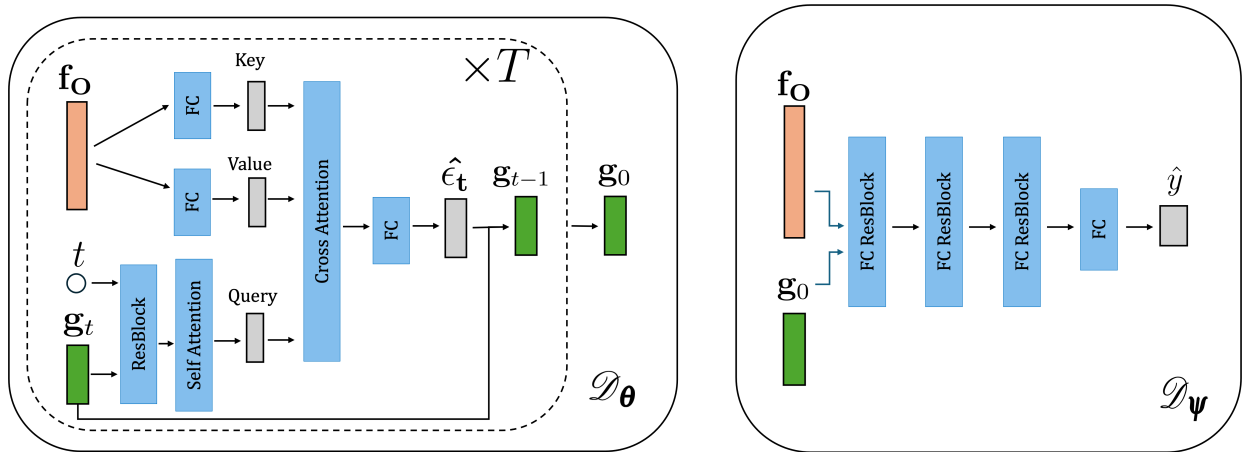


Fig. 2: **Model architecture.** The left image shows the DexSampler. Its input  $\mathbf{f}_O$  is processed into a key-value pair while  $\mathbf{g}_t$  at time  $t$  is processed into a query using a self-attention block. The key-value-query triplet is then embedded using a cross-attention block and used to compute  $\hat{\epsilon}_t$ . The right image shows the DexEvaluator that predicts grasp success probability given the same  $\mathbf{f}_O$  as the DexSampler and  $\mathbf{g}_0$  produced by the DexSampler.

of a Gaussian distribution. The parameters  $\theta$  are learned by minimizing the loss function

$$L_\epsilon = \|\hat{\epsilon}_t - \epsilon_t\|^2, \quad (3)$$

where  $\hat{\epsilon}_t$  is the noise estimated from  $\mathcal{N}(\hat{\mu}_t, \hat{\Sigma}_t)$  and  $\epsilon_t$  is the ground-truth noise at time  $t$ .

The architecture of DexSampler is depicted in Fig. 2, following the practical design of conditional diffusion model [6, 30, 32, 7]. It takes three inputs:  $\mathbf{f}_O$ ,  $\mathbf{g}_t$ , and  $t$  and outputs  $\hat{\epsilon}_t$  for grasp denoising.

To sample grasp using  $\epsilon_\theta$ , we define the conditional denoising process as follows:

$$p_\theta(\mathbf{g}_{0:T}|\mathbf{f}_O) = p(\mathbf{g}_T)\prod_{t=1}^T p_\theta(\mathbf{g}_{t-1}|\mathbf{g}_T, \mathbf{f}_O) \quad (4)$$

$$p_\theta(\mathbf{g}_{t-1}|\mathbf{g}_T, \mathbf{f}_O) = \mathcal{N}(\mathbf{g}_{t-1}; \hat{\mu}_t, \hat{\Sigma}_t). \quad (5)$$

Starting from  $\mathbf{f}_O$  and  $\mathbf{g}_T$ , DexSampler iteratively performs the denoising process  $T$  times to generate a high-quality grasp on the object.

### C. Grasp Evaluator

Although DexDiffuser is trained to generate successful grasps, it can still produce unsuccessful ones. It would be useful if we, before executing the grasp, could identify successful from unsuccessful grasps in order to only keep the successful ones. We propose the DexEvaluator  $\mathcal{D}_\psi(S=1|\mathbf{g} \in \mathbf{G}, \mathbf{f}_O)$  to do the task of predicting grasp success probability.

The architecture of DexEvaluator is adopted from [20] and shown in Fig. 2. It takes two inputs:  $\mathbf{g}$  and  $\mathbf{f}_O$  and outputs  $S$ . The parameters  $\psi$  of the DexEvaluator is optimized using the binary cross-entropy loss

$$L(y, \hat{y}) = -y \log(\hat{y}) + (1-y) \log(1-\hat{y}), \quad (6)$$

where  $y$  and  $\hat{y}$  denote the ground truth and predicted grasp labels, respectively. In Section V, we provide details on the dataset used to train DexEvaluator.

In addition to evaluating grasps, the DexEvaluator can also be used to guide the inverse diffusion process towards more successful grasps or refine already sampled grasps. This we discuss next.

### D. Grasp Refinement

The idea behind grasp refinement is to increase the probability of grasp success. In this work, we propose two grasp refinement strategies: EGD, which uses the evaluator to guide the inverse diffusion process, and ESR, which uses the evaluator to refine already sampled grasps.

1) *EGD*: EGD is a form of classifier-guided diffusion. Formally, during the inverse diffusion process, a noisy grasp  $\mathbf{g}_T$  at time  $t$  is iteratively denoised as

$$p_\theta(\mathbf{g}_{t-1}|\mathbf{g}_T, \mathbf{f}_O) = \mathcal{N}(\mathbf{g}_{t-1}; \mu_\theta(\mathbf{g}_T, t, \mathbf{f}_O) + \lambda \cdot \mathbf{g}_{\text{guide}}, \Sigma_\theta(\mathbf{g}_T, t, \mathbf{f}_O)), \quad (7)$$

$$\mathbf{g}_{\text{guide}} = \nabla_{\mathbf{g}_t} \log \mathcal{D}_\psi(\hat{y} = 1|\mathbf{g}_t, \mathbf{f}_O) + \log(T-t+1), \quad (8)$$

where  $\mathbf{g}_{\text{guide}}$  is the gradient signal from DexEvaluator modulated by  $\log(T-t+1)$ . In each step of the inverse diffusion process,  $\mathbf{g}_{\text{guide}}$  is used to adjust  $\mu_\theta$  towards more successful grasp. The magnitude of the adjustment is controlled by the parameter  $\lambda$ . The time-dependent modulation term  $\log(T-t+1)$  ensures that the guidance is more pronounced in the earlier stages of denoising when the uncertainty in the grasp is higher.

2) *ESR*: Compared to EGD, ESR locally refines already sampled grasps. Prior research on parallel-jaw grasp sampling [22] has demonstrated that many sampled grasps with low evaluator scores often lie spatially close to higher-scoring ones, suggesting that local grasp refinement can improve the grasp success probability. Building upon this insight, we extend the concept of local refinement for parallel-jaw grasps [22, 23] to dexterous grasps, which requires us to refine  $\mathbf{p}$ ,  $\mathbf{r}$  and  $\mathbf{q}$ .

Mathematically, local grasp refinement boils down to finding a  $\Delta \mathbf{g}$  so that  $P(S=1|\mathbf{g} + \Delta \mathbf{g}, \mathbf{f}_O) > P(S=1|\mathbf{g}, \mathbf{f}_O)$ . To find

$\Delta\mathbf{g}$ , we use the Metropolis-Hasting (MH) sampling algorithm as it has been shown to perform well for refining parallel-jaw grasps [23]. To apply MH, we first sample  $\Delta\mathbf{g}$  from a known probability distribution and then calculate the acceptance ratio  $\alpha = \frac{\mathcal{P}_{\Psi}(S=1|\mathbf{g}+\Delta\mathbf{g},\mathbf{f}_0)}{\mathcal{P}_{\Psi}(S=1|\mathbf{g},\mathbf{f}_0)}$ . If  $\alpha \geq u$ , where  $u \sim \mathcal{U}[0, 1]$ , then  $\mathbf{g} = \mathbf{g} + \Delta\mathbf{g}$  otherwise  $\mathbf{g}$  is not updated. We refer to this process as ESR-1, as it performs refinement simultaneously for every element of  $\mathbf{g}$ .

Because of the higher dimensional search space, local refinement is more challenging for dexterous than parallel-jaw grasps. Therefore, to make the refinement process more tractable, we introduce a two-stage ESR (ESR-2) that first refines  $\mathbf{r}$  and  $\mathbf{p}$  jointly and only afterward refines  $\mathbf{q}$ . The idea behind ESR-2 is first to refine the global grasp parameters  $\mathbf{r}$  and  $\mathbf{p}$  and only when these are good, refine the local parameters  $\mathbf{q}$ .

### E. Implementation Details

For training DexSampler, the hyperparameter  $\beta_t$  is controlled using a linear scheduler that moves from 0.0001 to 0.01 over a total of 100 timesteps. The learning rate is initially set to 1e-4 and controlled by an exponential rate scheduler with  $\gamma = 0.9$ . DexSampler is trained with a batch size of 16384 for 200 epochs.

The learning rate for the DexEvaluator is also set to 1e-4 but controlled with a plateau scheduler. The DexEvaluator is trained with a batch size of 25600 object-grasp pairs for 30 epochs.

For calculating the BPS we randomly sample one set of 4096 basis points. This one set is then used to calculate the BPS for every  $\mathbf{O}$  in the dataset.

## V. DATASET

For training DexSampler, we need a dataset that only includes successful dexterous grasps on partially occluded point clouds. For this purpose, we use the MultiDex dataset [9] that consists of 42 objects and 37774 grasps. We render 100 different  $\mathbf{O}$  for each object in the Isaac gym simulation [18].

In comparison, training DexEvaluator requires a dataset that includes both successful and unsuccessful grasps. Unfortunately, all current publicly available dexterous grasping datasets, including MultiDex, only contain successful grasps. However, instead of collecting a completely new dataset, we propose Algorithm 1 to extend existing datasets with unsuccessful grasps. Specifically, for every successful object-grasp pair  $(\mathbf{O}_k, \mathbf{g}_k)$  in the original dataset  $\Omega^{suc}$ , we generate three additional grasps  $\mathbf{g}_k^{pert}$ ,  $\mathbf{g}_k^{noise}$ , and  $\mathbf{g}_k^D$  (line 3-5). The Isaacgym annotator then labels these new grasps for the expanded dataset  $\Omega_{label}^{cu}$ . To balance the number of successful and failed grasps, we randomly remove some successful pairs from  $\Omega_{label}^{cu}$ .

By applying Algorithm 1 on all of the 42 MultiDex objects, we collected an additional 26956 successful and 48644 unsuccessful grasps. We split this extended dataset into a training set consisting of 35 objects and a test set of 7. We further expand the test dataset with 49 objects from the EGAD!

---

## Algorithm 1: Grasp Curation

---

**Data:**  $N$  successful object-grasp data pairs  
 $\Omega^{suc} = \{(\mathbf{O}_1, \mathbf{g}_1), \dots, (\mathbf{O}_N, \mathbf{g}_N)\}$ , DexDiffuser  $\mathcal{D}_\theta$ , an Isaacgym annotator  $D_{isaac}$ , a object mesh database  $\mathbf{M}_{object}$

**Result:** Curated dataset  $\Omega_{label}^{cu}$

- 1 Initialize  $\Omega^{cu} = \emptyset$ , Initialize  $\Omega_{label}^{cu} = \emptyset$
- 2 **for**  $k = 1$  to  $N$  **do**
- 3      $\mathbf{g}_k^{pert} = \mathbf{g}_k + \Delta\mathbf{g}_k$ , where  $\Delta\mathbf{g}_k$  is a grasp perturbation
- 4      $\mathbf{g}_k^{noise} = \mathcal{D}_\theta(\mathbf{O}_{noise})$ , where  $\mathbf{O}_{noise}$  is a random noisy point cloud
- 5      $\mathbf{g}_k^D = \mathcal{D}_\theta(\mathbf{O}_k)$
- 6     Retrieve the object mesh  $\mathbf{M}_k$  for  $\mathbf{O}_k$  from  $\mathbf{M}_{object}$
- 7      $\Omega^{cu} := \Omega^{cu} \cup \{(\mathbf{M}_k, \mathbf{O}_k, \mathbf{g}_k), (\mathbf{M}_k, \mathbf{O}_k, \mathbf{g}_k^{pert}), (\mathbf{M}_k, \mathbf{O}_k, \mathbf{g}_k^D), (\mathbf{M}_k, \mathbf{O}_k, \mathbf{g}_k^{noise})\}$
- 8 **end**
- 9 **for**  $(\mathbf{M}_i, \mathbf{O}_i, \mathbf{g}_i) \in \Omega^{cu}$  **do**
- 10      $y_i = D_{isaac}(\mathbf{M}_i, \mathbf{g}_i)$
- 11      $\Omega_{label}^{cu} := \Omega_{label}^{cu} \cup \{(\mathbf{O}_i, \mathbf{g}_i, y_i)\}$
- 12 **end**
- 13 **Return**  $\Omega_{label}^{cu}$

---

dataset [21] and 12 objects from the KIT dataset [8]. Again, we applied Algorithm 1 on the added test objects, but, as no prior dexterous grasps exist for them, we skipped line 3 in Algorithm 1. Finally, we rendered 10 different  $\mathbf{O}$  of each object in the expanded evaluator dataset.

## VI. EXPERIMENTAL EVALUATION

We experimentally evaluated DexDiffuser in both simulation and the real world, comparing it to the state-of-the-art method FFHNet [20]. The specific questions we wanted to address with the experiments were:

- 1) What effect does the BPS-encoding have on generating successful grasps?
- 2) How well can the DexEvaluator predict grasp success?
- 3) To what extent do ESR and EGD improve the grasp quality?
- 4) How well can DexDiffuser generalize to real-world object grasping?

### A. Simulation Experiments

All simulation experiments were conducted in Isaac Gym [18] following the setup from [9]. Specifically, test objects were initialized as free-floating objects, and a virtual 16-DoF Allegro Hand was used for grasping each of them. For each of the 68 test objects, 10 point clouds were rendered from randomly sampled camera poses. Then, all methods generated 20 grasps per point cloud, which amounted to 13,600 test grasps per method. Once an object was grasped, the grasp stability was assessed by applying external forces along the six directions in space for 50 timesteps. A grasp succeeded if the object remained in the hand throughout the stability test.

We also trained a DexSampler with the PointNet++ point cloud encoding [28] to study what effect different encodings had on grasp performance. We call that network DexDiffuser-PN2 while the BPS network is referred to as DexDiffuser-BPS.

1) *Grasp Sampling:* To address the first question, we evaluated both FFHNet and DexSampler using the PointNet++ or BPS encoding. The simulation results are presented in Table I.

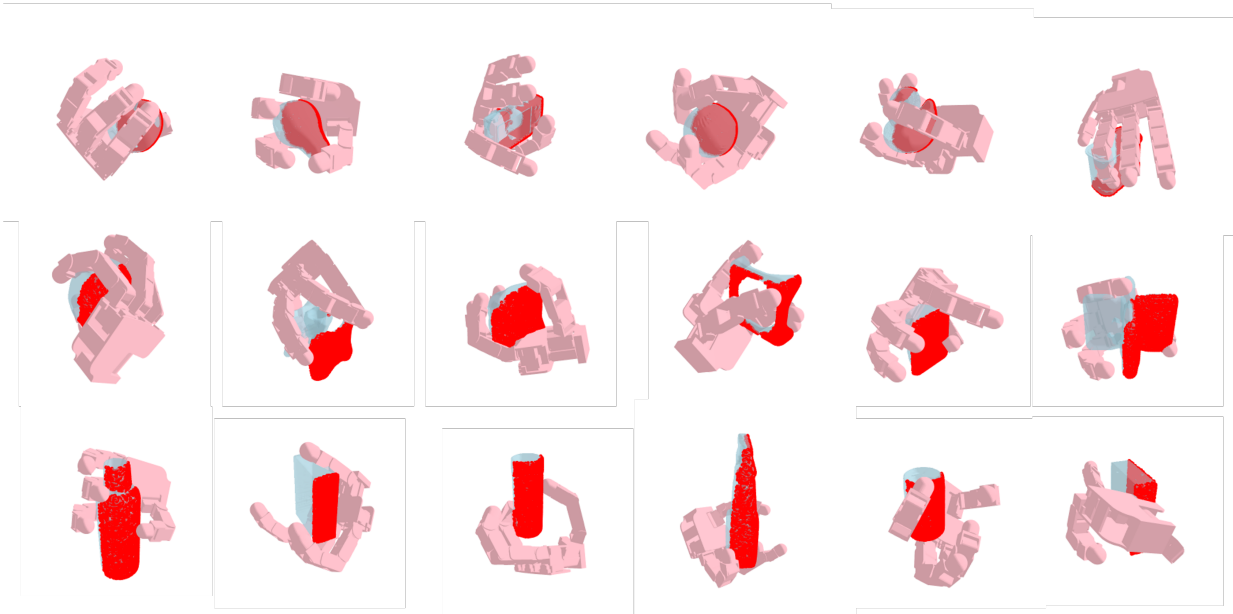


Fig. 3: Qualitative evaluation of DexSampler-BPS on objects from MultiDex (top row), EGAD! (middle row), and KIT (bottom row). The grasps, shown in pink, are generated on the partially observed point clouds, shown in red. The point clouds are rendered from the complete meshes, shown in blue.

Method	Dataset		
	MultiDex(%) $\uparrow$	EGAD! (%) $\uparrow$	KIT (%) $\uparrow$
FFHNet [20]	61.64	63.14	53.91
DexS-PN2	87.07	81.59	54.54
DexS-BPS	<b>90.64</b>	<b>87.93</b>	<b>75.00</b>
FFHNet-ESR-1	64.64	65.66	55.67
FFHNet-ESR-2	66.07	65.02	55.38
DexS-PN2-ESR-1	87.21	81.60	55.04
DexS-PN2-ESR-2	87.29	81.69	55.92
DexS-BPS-ESR-1	90.93	87.26	74.13
DexS-BPS-ESR-2	91.29	87.37	75.33
DexS-BPS-EGD	90.50	<b>88.01</b>	75.13
DexS-BPS-EGD-ESR-1	90.50	87.43	75.21
DexS-BPS-EGD-ESR-2	<b>91.43</b>	87.63	<b>76.08</b>

TABLE I: Grasp success rate of different methods. The three first rows exclude grasp refinement, while the bottom nine include it.  $\uparrow$ : The higher, the better. DexS represents the DexSampler.

These results demonstrate that DexSampler, irrespective of the encoding method, consistently outperformed the FFHNet generator across all tested datasets. The superior performance underscores the diffusion models’ effectiveness in synthesizing successful grasps. Moreover, DexSampler-BPS performed much better than DexSampler-PN2, indicating that the BPS

Dataset	Recall Pos. (%) $\uparrow$	Recall Neg. (%) $\uparrow$	Total Acc. (%) $\uparrow$
MultiDex val	86.50	89.97	88.68
EGAD!	68.80	74.78	69.99
KIT	65.93	72.78	69.04

TABLE II: Grasp success prediction result.  $\uparrow$ : The higher, the better.

encoding is less affected by point cloud irregularities, including missing parts and non-uniform density distribution. Finally, Fig. 3 shows some grasps generated by the DexSampler-BPS on the three datasets.

2) *Grasp Evaluation*: To answer the second question, we assessed the DexEvaluator’s grasp prediction accuracy. The results are presented in Table II and indicate that the DexEvaluator performed well on the MultiDex dataset but notably worse on the EGAD! and KIT datasets. The main reason for the performance decline is the geometric differences between the objects in the MultiDex dataset and those in the EGAD! and KIT datasets. As shown in Fig. 4, the objects in KIT are notably taller than those in MultiDex, while the objects in EGAD! have more complex geometry.

3) *Grasp Refinement*: To answer question 3, we assessed the impact grasp refinement had on the grasp success rate. The results, presented in Table II, show that ESR significantly improves grasp success rate, especially for the FFHNet. For the diffusion-based models, ESR and EGD showed only marginal improvements, which is consistent with findings reported in [11]. The two-stage refinement process ESR-2 consistently outperformed ESR-1, with the exception of FFHNet-ESR-2 on the EGAD! and KIT datasets.

We also evaluated the combination of EGD and ESR (EGD-ESR) on DexDiffuser by first applying EGD followed by ESR. Although the combination did achieve the highest grasp success rate on the MultiDex and KIT datasets, the improvement is, again, marginal compared to the other methods. We hypothesize that the performance is primarily limited by the DexEvaluator’s classification accuracy.

Real-world experiment Object	# of successful grasps per method and object					
	FFHNet	FFHNet-ESR-2	DexS-BPS	DexS-BPS-ESR-2	DexS-BPS-EGD	DexS-BPS-EGD-ESR-2
1. Cracker box	1/5	1/5	1/5	4/5	1/5	2/5
2. Sugar box	2/5	2/5	2/5	4/5	0/5	3/5
3. Mustard bottle	0/5	3/5	1/5	3/5	2/5	2/5
4. Bleach cleanser	2/5	2/5	4/5	5/5	2/5	2/5
5. Sprayer	2/5	3/5	2/5	4/5	3/5	2/5
6. Metal mug	1/5	1/5	3/5	3/5	2/5	2/5
7. Goblet	2/5	2/5	2/5	4/5	4/5	2/5
8. Toy plane	0/5	0/5	0/5	1/5	0/5	0/5
9. Pringles	1/5	2/5	3/5	3/5	3/5	2/5
Avg. success rate	24.44%	35.56%	40.00%	<b>68.89%</b>	37.78%	37.78%

TABLE III: Experimental results for real-world grasping. DexS represents DexSampler.

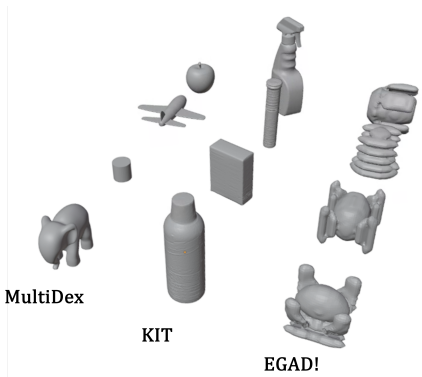


Fig. 4: Examples from the MultiDex, EGAD!, and KIT datasets.



Fig. 5: Experimental objects. From 1 to 9: cracker box, sugar box, mustard bottle, bleach cleanser, sprayer, metal mug, goblet, toy plane, and pringles

### B. Real Robot Experiment

To answer the last question, we evaluated how successful DexDiffuser was at picking objects from real noisy object point clouds using real robotic hardware. The hardware used is shown in Fig. 1 and includes an Allegro Hand attached to the end of a Franka Panda robot and a Kinect V3 placed in a third-person perspective to capture  $\mathbf{O}$ . We used a motion capture system to do the extrinsic camera calibration.

We chose 9 different test objects, all shown in Fig. 5, based on their variation in shape and size. Each object was placed in the robot’s workspace in five distinct orientations:  $0^\circ$ ,  $90^\circ$ ,  $120^\circ$ ,  $180^\circ$ , and  $240^\circ$ . All methods generated and ranked 200 grasps per object and orientation. Of these grasps, the best kinematically feasible one was executed on the robot. A grasp was successful if the robot picked the object and kept it grasped while moving to a predefined pose where it rotated the last joint  $\pm 90^\circ$ .

We evaluated the following methods: FFHNet, FFHNet-ESR-2, DexDiffuser-BPS, DexDiffuser-BPS-ESR-2. It is worth highlighting that all of these methods are only trained on simulated data.

The experimental results are summarized in Table III. Like the simulation results, these results show that DexDiffuser consistently outperformed FFHNet across all test objects. The best method for picking real-world objects was DexSampler-BPS-ESR-2, and some of the grasps it produced are shown in

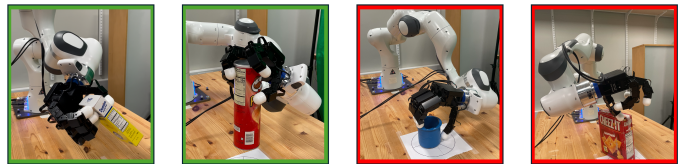


Fig. 6: Successful and failed grasp examples from DexSampler-BPS-ESR-2. The first two images are successful grasps for the sugar box and the pringles, while the latter two show different failure cases on the metal mug and the cracker box.

Fig. 6. However, in contrast to the simulation results, the real-world experiments revealed that doing no gripper refinement is better than EGD and EGD-ESR-2 refinement. We hypothesize that the performance drop is because EGD is sensitive to noisy point clouds, as only performing ESR-2 refinement achieved the best results.

The real-world results also indicated a significantly lower average grasp success rate than in simulation. One rather obvious reason for the decline in performance is that grasps generated on real noisy point clouds are poorer than those generated on clean simulated point clouds. Another reason is the presence of obstacles that impede the robot’s ability to attain the desired target position. For instance, the first failed grasp in Fig. 6 is because the gripper collided with the table when closing, while the second failure is because the robot

could not reach the intended grasp position due to joint limits. Neither of these failure cases is present in the simulation.

## VII. LIMITATIONS

Our work has three known limitations. The first is that the datasets used for training do not include enough tall and geometrically challenging objects as accentuated by the performance degradation on the EGAD! and KIT objects. The second limitation is the performance degradation from sim-to-real. The final limitation is that neither the sampler nor the evaluator accounts for environmental constraints such as the table or other collision objects.

## VIII. CONCLUSION

This paper addressed the problem of dexterous grasping under partial point cloud observations. Our proposed solution, DexDiffuser, consisted of a conditional diffusion-based grasp sampler and grasp evaluator, BPS-encoded point clouds, and two different grasp refinement strategies. All simulation and real-world experiments on the 16-DoF Allegro hand demonstrated that DexDiffuser consistently outperformed FFHNet with an, on average, 21.71–22.20% higher grasp success rate.

On its own, this work represents one of the few data-driven dexterous grasping methods that can generate grasps directly from partial point clouds and is evaluated on real hardware. Based on the improvements that the diffusion model brought, we believe it can be used to solve other challenging dexterous manipulation tasks such as in-hand manipulation, dexterous grasping in clutter, and joint motion and dexterous grasp planning. Addressing these challenges and the limitations of our method highlights promising future research directions.

## REFERENCES

- [1] Joao Carvalho, An T Le, Mark Baiert, Dorothea Koert, and Jan Peters. Motion planning diffusion: Learning and planning of robot motions with diffusion models. In *2023 IEEE/RSJ International Conference on Intelligent Robots and Systems (IROS)*, pages 1916–1923. IEEE, 2023.
- [2] Lili Chen, Shikhar Bahl, and Deepak Pathak. Playfusion: Skill acquisition via diffusion from language-annotated play. In *Conference on Robot Learning*, pages 2012–2029. PMLR, 2023.
- [3] Cheng Chi, Siyuan Feng, Yilun Du, Zhenjia Xu, Eric Cousineau, Benjamin Burchfiel, and Shuran Song. Diffusion policy: Visuomotor policy learning via action diffusion. In *Proceedings of Robotics: Science and Systems (RSS)*, 2023.
- [4] Changhyun Choi, Wilko Schwarting, Joseph DelPreto, and Daniela Rus. Learning object grasping for soft robot hands. *IEEE Robotics and Automation Letters*, 3(3): 2370–2377, 2018.
- [5] Jonathan Ho and Tim Salimans. Classifier-free diffusion guidance. *arXiv preprint arXiv:2207.12598*, 2022.
- [6] Jonathan Ho, Chitwan Saharia, William Chan, David J Fleet, Mohammad Norouzi, and Tim Salimans. Cascaded diffusion models for high fidelity image generation. *The*

- Journal of Machine Learning Research*, 23(1):2249–2281, 2022.
- [7] Siyuan Huang, Zan Wang, Puhao Li, Baoxiong Jia, Tengyu Liu, Yixin Zhu, Wei Liang, and Song-Chun Zhu. Diffusion-based generation, optimization, and planning in 3d scenes. In *Proceedings of the IEEE/CVF Conference on Computer Vision and Pattern Recognition*, pages 16750–16761, 2023.
- [8] Alexander Kasper, Zhixing Xue, and Rüdiger Dillmann. The kit object models database: An object model database for object recognition, localization and manipulation in service robotics. *The International Journal of Robotics Research*, 31(8):927–934, 2012.
- [9] Puhao Li, Tengyu Liu, Yuyang Li, Yixin Zhu, Yaodong Yang, and Siyuan Huang. Gendexgrasp: Generalizable dexterous grasping. *arXiv preprint arXiv:2210.00722*, 2022.
- [10] Min Liu, Zherong Pan, Kai Xu, Kanishka Ganguly, and Dinesh Manocha. Generating grasp poses for a high-dof gripper using neural networks. In *2019 IEEE/RSJ International Conference on Intelligent Robots and Systems (IROS)*, pages 1518–1525. IEEE, 2019.
- [11] W Liu, Y Du, T Hermans, S Chernova, and C Paxton. Structdiffusion: Language-guided creation of physically-valid structures using unseen objects. In *RSS*, volume 1, page 3, 2023.
- [12] Weiyu Liu, Yilun Du, Tucker Hermans, Sonia Chernova, and Chris Paxton. Structdiffusion: Language-guided creation of physically-valid structures using unseen objects. In *Proceedings of Robotics: Science and Systems (RSS)*, 2023.
- [13] Jiaxin Lu, Hao Kang, Haoxiang Li, Bo Liu, Yiding Yang, Qixing Huang, and Gang Hua. Ugg: Unified generative grasping, 2023.
- [14] Qingkai Lu, Mark Van der Merwe, and Tucker Hermans. Multi-fingered active grasp learning. In *2020 IEEE/RSJ International Conference on Intelligent Robots and Systems (IROS)*, pages 8415–8422. IEEE, 2020.
- [15] Qingkai Lu, Mark Van der Merwe, Balakumar Sundaralingam, and Tucker Hermans. Multifingered grasp planning via inference in deep neural networks: Outperforming sampling by learning differentiable models. *IEEE Robotics & Automation Magazine*, 27(2):55–65, 2020.
- [16] Jens Lundell, Enric Corona, Tran Nguyen Le, Francesco Verdoja, Philippe Weinzaepfel, Grégory Rogez, Francesc Moreno-Noguer, and Ville Kyrki. Multi-fingan: Generative coarse-to-fine sampling of multi-finger grasps. In *2021 IEEE International Conference on Robotics and Automation (ICRA)*, pages 4495–4501. IEEE, 2021.
- [17] Jens Lundell, Francesco Verdoja, and Ville Kyrki. Ddgc: Generative deep dexterous grasping in clutter. *IEEE Robotics and Automation Letters*, 6(4):6899–6906, 2021. doi: 10.1109/LRA.2021.3096239.
- [18] Viktor Makoviychuk, Lukasz Wawrzyniak, Yunrong Guo, Michelle Lu, Kier Storey, Miles Macklin, David

- Hoeller, Nikita Rudin, Arthur Allshire, Ankur Handa, et al. Isaac gym: High performance gpu-based physics simulation for robot learning. *arXiv preprint arXiv:2108.10470*, 2021.
- [19] Priyanka Mandikal and Kristen Grauman. Dexterous robotic grasping with object-centric visual affordances. In *International Conference on Robotics and Automation (ICRA)*, 2021.
- [20] Vincent Mayer, Qian Feng, Jun Deng, Yunlei Shi, Zhaopeng Chen, and Alois Knoll. Ffhnet: Generating multi-fingered robotic grasps for unknown objects in real-time. In *2022 International Conference on Robotics and Automation (ICRA)*, pages 762–769, 2022. doi: 10.1109/ICRA46639.2022.9811666.
- [21] Douglas Morrison, Peter Corke, and Jürgen Leitner. Egad! an evolved grasping analysis dataset for diversity and reproducibility in robotic manipulation. *IEEE Robotics and Automation Letters*, 5(3):4368–4375, 2020.
- [22] Arsalan Mousavian, Clemens Eppner, and Dieter Fox. 6-dof graspnet: Variational grasp generation for object manipulation. In *International Conference on Computer Vision (ICCV)*, 2019.
- [23] Adithyavairavan Murali, Arsalan Mousavian, Clemens Eppner, Chris Paxton, and Dieter Fox. 6-dof grasping for target-driven object manipulation in clutter. In *2020 IEEE International Conference on Robotics and Automation (ICRA)*, pages 6232–6238. IEEE, 2020.
- [24] Rhys Newbury, Morris Gu, Lachlan Chumbley, Arsalan Mousavian, Clemens Eppner, Jürgen Leitner, Jeannette Bohg, Antonio Morales, Tamim Asfour, Danica Kragic, et al. Deep learning approaches to grasp synthesis: A review. *IEEE Transactions on Robotics*, 2023.
- [25] Eley Ng, Ziang Liu, and Monroe Kennedy. Diffusion co-policy for synergistic human-robot collaborative tasks. *IEEE Robotics and Automation Letters*, 2023.
- [26] Simon Ottenhaus, Daniel Renninghoff, Raphael Grimm, Fabio Ferreira, and Tamim Asfour. Visuo-haptic grasping of unknown objects based on gaussian process implicit surfaces and deep learning. In *2019 IEEE-RAS 19th International Conference on Humanoid Robots (Humanoids)*, pages 402–409. IEEE, 2019.
- [27] Sergey Prokudin, Christoph Lassner, and Javier Romero. Efficient learning on point clouds with basis point sets. In *Proceedings of the IEEE/CVF international conference on computer vision*, pages 4332–4341, 2019.
- [28] Charles Ruizhongtai Qi, Li Yi, Hao Su, and Leonidas J Guibas. Pointnet++: Deep hierarchical feature learning on point sets in a metric space. *Advances in neural information processing systems*, 30, 2017.
- [29] Yuzhe Qin, Binghao Huang, Zhao-Heng Yin, Hao Su, and Xiaolong Wang. Dexpoint: Generalizable point cloud reinforcement learning for sim-to-real dexterous manipulation, 2022.
- [30] Robin Rombach, Andreas Blattmann, Dominik Lorenz, Patrick Esser, and Björn Ommer. High-resolution image synthesis with latent diffusion models. In *Proceedings of the IEEE/CVF conference on computer vision and pattern recognition*, pages 10684–10695, 2022.
- [31] Hyunwoo Ryu, Jiwoo Kim, Junwoo Chang, Hyun Seok Ahn, Joohwan Seo, Taehan Kim, Jongeun Choi, and Roberto Horowitz. Diffusion-edfs: Bi-equivariant denoising generative modeling on  $se(3)$  for visual robotic manipulation. *arXiv preprint arXiv:2309.02685*, 2023.
- [32] Chitwan Saharia, William Chan, Saurabh Saxena, Lala Li, Jay Whang, Emily L Denton, Kamyar Ghasemipour, Raphael Gontijo Lopes, Burcu Karagol Ayan, Tim Salimans, et al. Photorealistic text-to-image diffusion models with deep language understanding. *Advances in Neural Information Processing Systems*, 35:36479–36494, 2022.
- [33] Anthony Simeonov, Ankit Goyal, Lucas Manuelli, Lin Yen-Chen, Alina Sarmiento, Alberto Rodriguez, Pulkit Agrawal, and Dieter Fox. Shelving, stacking, hanging: Relational pose diffusion for multi-modal rearrangement. *Conference on Robot Learning*, 2023.
- [34] Julen Urain, Niklas Funk, Jan Peters, and Georgia Chalvatzaki. Se (3)-diffusionfields: Learning smooth cost functions for joint grasp and motion optimization through diffusion. In *2023 IEEE International Conference on Robotics and Automation (ICRA)*, pages 5923–5930. IEEE, 2023.
- [35] Mark Van der Merwe, Qingkai Lu, Balakumar Sundaralingam, Martin Matak, and Tucker Hermans. Learning continuous 3d reconstructions for geometrically aware grasping. In *2020 IEEE International Conference on Robotics and Automation (ICRA)*, pages 11516–11522. IEEE, 2020.
- [36] Weikang Wan, Haoran Geng, Yun Liu, Zikang Shan, Yaodong Yang, Li Yi, and He Wang. Unidexgrasp++: Improving dexterous grasping policy learning via geometry-aware curriculum and iterative generalist-specialist learning, 2023.
- [37] Wei Wei, Daheng Li, Peng Wang, Yiming Li, Wanyi Li, Yongkang Luo, and Jun Zhong. Dvvg: Deep variational grasp generation for dextrous manipulation. *IEEE Robotics and Automation Letters*, 7(2):1659–1666, 2022.
- [38] Albert Wu, Michelle Guo, and Karen Liu. Learning diverse and physically feasible dexterous grasps with generative model and bilevel optimization. In Karen Liu, Dana Kulic, and Jeff Ichnowski, editors, *Proceedings of The 6th Conference on Robot Learning*, volume 205 of *Proceedings of Machine Learning Research*, pages 1938–1948. PMLR, 14–18 Dec 2023.
- [39] Ling Yang, Zhilong Zhang, Yang Song, Shenda Hong, Runsheng Xu, Yue Zhao, Wentao Zhang, Bin Cui, and Ming-Hsuan Yang. Diffusion models: A comprehensive survey of methods and applications. *ACM Computing Surveys*, 56(4):1–39, 2023.
- [40] Yi Zhou, Connelly Barnes, Jingwan Lu, Jimei Yang, and Hao Li. On the continuity of rotation representations in neural networks. In *Proceedings of the IEEE/CVF Conference on Computer Vision and Pattern Recognition*, pages 5745–5753, 2019.